Microsyst Technol (2012) 18:1661–1667
DOI 10.1007/s00542-012-1607-9

TECHNICAL PAPER

Time dependent simulation of active flying height control of TFC sliders

Pablo Antonio Salas · Uwe Boettcher · Frank E. Talke

Received: 31 August 2011 / Accepted: 15 June 2012 / Published online: 4 July 2012

Abstract A time-dependent numerical simulation procedure is implemented to simulate the flying height response of a typical thermal flying height control (TFC) slider as a function of the power input to the heater element. The Reynolds equation is used in conjunction with a TFC slider finite element model to determine the change in the thermal protrusion and flying height of the slider. The power input signal to the heater element is optimized using convex optimization to minimize flying height variations of the slider. The optimization procedure is applied to a typical experimentally measured flying height profile. The numerical simulation results are in excellent qualitative agreement with experimental measurements.

1 Introduction

Thermal Flying-height Control (TFC) sliders have been recently used to reduce flying height at the head disk interface and obtain more stable flying heights (Kurita et al. 2005; Song et al. 2007; Liu et al. 2008). TFC sliders have a built-in resistance heater that causes a thermal deformation (protrusion) of the air bearing surface near the read-write element, which results in a reduction of the head disk spacing. TFC sliders were developed to compensate for thermal effects caused by the power input to the write head. It was recently shown by Boettcher et al. (2011) that active dynamic flying height control of a TFC slider in the 15 kHz range is possible using feed forward control and a second order dynamic model for the TFC heater. Determining the optimum time-varying power for the heater along the circumference of the disk, Boettcher et al. (2011) were able to reduce the flying height variations of the slider by a factor of three. Based on this work, it is apparent that dynamic flying height control of a TFC slider for best frequency response is highly desirable. The response of the heater is a thermal process that can be described by means of two time-constants: a short one for the short time response and a long one for the long time response. For high bandwidth real-time flying height control it is crucial that the initial response time be as short as possible. The purpose of this investigation is to simulate numerically the time dependent response of a TFC slider to a time-dependent power input to the heater. The time-dependent thermal protrusion of the slider contour due to time-dependent power changes of the TFC heater is determined and coupled with the Reynolds equation to investigate the dynamics of TFC sliders. Numerical results are compared with flying height time-dependent measurements based on feed forward control strategies.

2 Background

In Fig. 1, a typical result is shown from Boettcher et al. (2011) for the change of flying height of a TFC slider as a function of time for a constant heater input. We note that the change of flying height of the slider is a repeatable function of the position along the disk, with non-repeatable contributions of smaller magnitude superimposed on the repeatable flying height signal. In Boettcher et al. (2011) the current input to the heater was optimized to minimize

P. A. Salas (✉) · U. Boettcher · F. E. Talke
Center for Magnetic Recording Research, University of California, San Diego, 9500 Gilman Drive, #0401, La Jolla, CA 92093, USA
e-mail: psalasme@ucsd.edu

the flying height change using a feed forward control approach. The experimentally measured flying height profile using the optimized input to the heater is also shown in Fig. 1. In order to perform the optimization, the dynamics of the heater were estimated by measuring the transient response of the TFC slider to a step function. Figure 2 shows a typical experimental result for the change of flying height Δz as a function of time in response to a step change of the power input to the heater element. We observe that a transient flying height region is present prior to the slider reaching steady state. It was shown by Boettcher et al. (2011) that a second order model can capture the flying height response of the measured data as a function of time.

The procedure and results obtained by Boettcher et al. (2011) are data-based, and the question arises as to whether the change of flying height as a function of the current input to the heater element can be obtained using first principles, i.e., using the equations governing the flying characteristics and the thermal response of a typical TFC slider. The goal of this work is to numerically calculate the thermal protrusion of a typical TFC slider (Li et al. 2010; Fritzsche et al. 2011), determine the time-dependent response of the slider as a function of the time-dependent heater input signal, and compare the numerical results with the experimental data presented by Boettcher et al. (2011).

3 Problem governing equations

The air flow at the head disk interface is governed by the steady state Reynolds equation (Wahl et al. 1996).

$$\nabla \times (Qph^3\nabla p) = 6\mu U \times \nabla(ph) \tag{1}$$

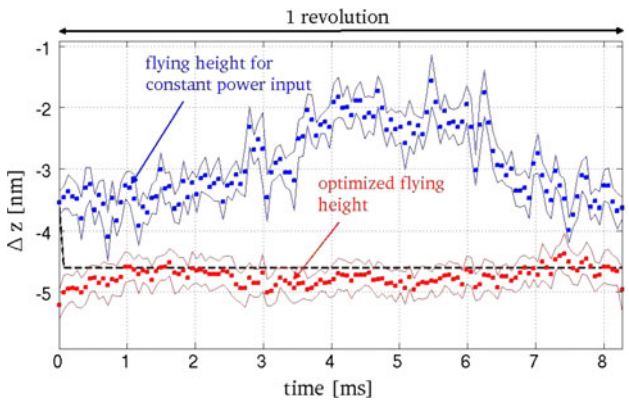

Fig. 1 Experimentally measured flying height profiles due to constant and optimized power input to the heater element. The *square symbols* represent the mean of 20 measurements. The *solid lines* represent one standard deviation confidence intervals for each set of measurements. Source: Boettcher et al. (2011)

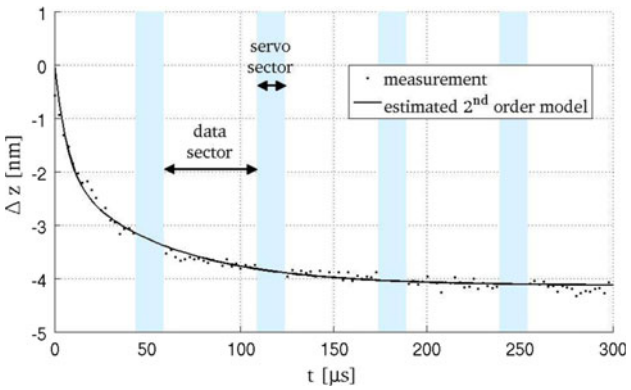

Fig. 2 Flying height change Δz due to a step power input to the heater element. Source: Boettcher et al. (2011)

where p represents pressure, h the spacing between slider and disk, Q is the rarefaction term, μ the viscosity and U the velocity of the disk. In Eq. 1, the pressure terms on the left equal the viscous terms on the right. The slider equilibrium equations (Duwensee 2007) represent the balance between air bearing forces and external suspension forces. The equilibrium equations are given by

$$\begin{aligned} \iint_A p(x,y)dA + F_z &= 0 \\ \iint_A p(x,y)(x-x_p)dA + M_\alpha &= 0 \\ \iint_A p(x,y)(y-y_p)dA + M_\beta &= 0 \end{aligned} \tag{2}$$

where x_p represents the x coordinate of the slider pivot point, y_p the y coordinate of the slider pivot point, F_z the external force in the vertical direction, M_α the external moment in the pitch direction and M_β the external moment in the roll direction. Heat conduction has been shown to be the dominant heat transfer process between the slider and the air bearing (Zhang and Bogy 1999). Therefore, the heat flux between the slider and the air bearing can be computed as follows (Zhou et al. 2008)

$$q(x) = -k\frac{T_d - T_s}{h(x) + 2b\lambda(x)} \tag{3}$$

where k represents the thermal conductivity of the air, T_s and T_d the temperatures of the slider and the disk, respectively, h the spacing between slider and disk, λ the local mean free path of air, b a constant equal to $b = 2(2 - \sigma_T)\gamma/(\sigma_T(\gamma + 1)Pr)$, σ_T the thermal accommodation coefficient, γ the ratio of the specific heat and Pr the Prandtl number. The heat flux is a function of the flying height, which is computed using the Reynolds equation and slider equilibrium equations.

4 Steady state numerical simulation

The following iterative procedure can be used to determine the steady state solution of TFC sliders (Li et al. 2010; Fritzsche et al. 2011). First, the steady state Reynolds equation and slider equilibrium equations are solved to determine the air bearing pressure and the flying height of the slider. The computed pressure and flying height are then used to calculate the heat transfer coefficient profile from the slider to the air bearing surface using the generalized heat flux model presented in Eq. 3. The computed heat transfer coefficients serve as convection boundary conditions for the TFC slider finite element model. A coupled thermal structural finite element analysis is then performed to determine the change in thermal protrusion of the TFC slider. At each time step, the TFC slider geometry is updated and the air bearing pressure and flying height are computed again. The entire process is repeated until the equilibrium position of the slider is achieved for a fixed power input.

5 TFC slider finite element model

The TFC slider finite element model was implemented using the LS-DYNA finite element code (Livermore Software Technology Corporation 2007). The material properties and geometric dimensions of the TFC slider finite element model are presented in Table 1 and Fig. 3, respectively. As discussed in the previous section, the heat transfer coefficient between the air bearing and the slider is used as a boundary condition for the TFC slider model. Therefore, the heat transfer coefficient values have to be mapped to the TFC slider finite element model. The heat transfer coefficient values were interpolated to the TFC slider finite element mesh using the known values at the nodes of the air bearing surface model mesh. Shape type functions similar to those employed in finite element formulations were used at the element level to linearly interpolate the heat transfer coefficient values among the nodes. The TFC slider finite element model was validated using existing thermal protrusion results for steady state conditions and showed excellent agreement with the data.

6 Time-dependent simulation using steady state Reynolds equation solver

If the power input to the TFC slider is changed as a function of time, as would occur in the case of active flying height control situations, the time-dependent Reynolds equation must be used to determine the transient response of the TFC slider. Since the air bearing reaches equilibrium (steady state) much faster than the slider reaches its thermal equilibrium, the quasi-steady approach presented in Fig. 4 can be used. We first calculate the thermal deformation for a given power input at a fixed time step and use the steady state Reynolds equation solver to iterate at this time step until equilibrium is reached using the numerical procedure described in the previous sections. We then advance to the next time step where the power input might have changed. At the new time step, we again determine the air bearing pressure and flying height from the steady state Reynolds equation, and iterate at this fixed time step, with constant power input, until the equilibrium position of the slider is obtained. This procedure is repeated for each time step until convergence is reached, resulting in flying height changes as a function of time for the chosen input power signal.

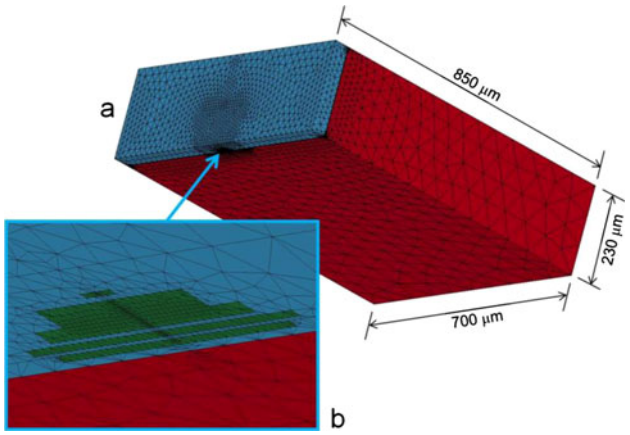

Fig. 3 Finite element model of (**a**) TFC slider and (**b**) read-write element

Table 1 Material properties of TFC slider finite element model

Materials	Young's modulus (GPa)	Poisson's ratio	Coefficient of thermal expansion	Thermal conductivity (W/mK)
Al_2O_3TiC	390	0.22	7.1e-6	20
Al_2O_3	138	0.25	7.1e-6	18
NiFe (pole, shield)	200	0.3	12.8e-6	35
Cu (write coil)	130	0.34	15.4e-6	403
NiCr (heater)	200	0.3	17e-6	15
Resist	3.8	0.35	31e-6	0.1

7 Numerical simulation of flying height changes

In the experimental work highlighted at the beginning of this paper, flying height changes were experimentally measured by using the read back signal in the hard drive. In the numerical simulation, the calculated flying height for a constant heater input resembles a straight line as the thermal process approaches equilibrium, as can be seen in Fig. 5. In order to simulate the flying height changes observed in the experimental measurements shown in Fig. 1, it is necessary to introduce flying height variations to the computed flying height. The experimental data shown in Fig. 1 (sampled at approximately 15 kHz across one disk revolution) was used to simulate the variations. The experimental flying height variations were added to the computed steady state flying height of the slider to obtain the flying height profile shown in Fig. 5.

8 TFC slider dynamics

In order to minimize the flying height change shown in Fig. 5, the power input to the heater element must be optimized as a function of time to generate the thermal protrusion needed to minimize the change of flying height. In order to carry out the optimization, a discrete time model of the thermal actuator must be determined. The generalized realization algorithm (GRA) (de Callafon et al. 2008) can be used to identify the heater actuator dynamics. The general methodology of GRA is briefly discussed next. The input to output relationship of the TFC heater system can be expressed as:

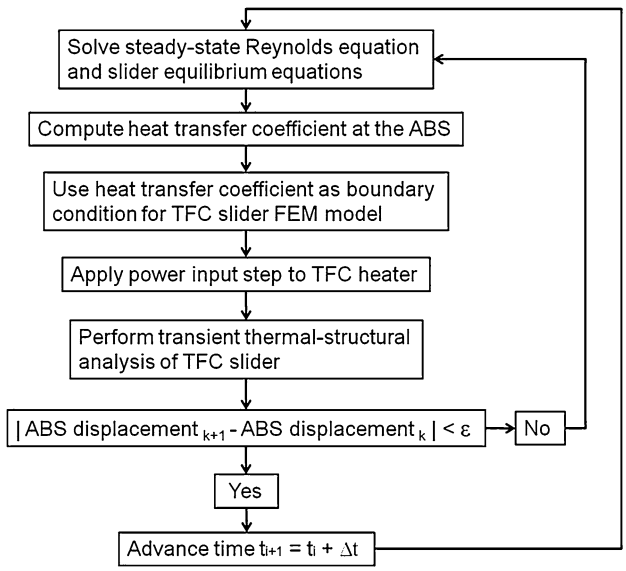

Fig. 4 Schematic representation of time dependent simulation of TFC slider response

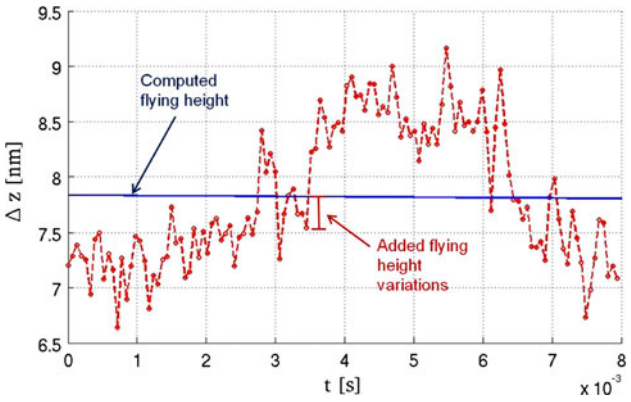

Fig. 5 Flying height variations (*dotted points*) were added to the computed steady state flying height (*solid line*) to simulate a flying height profile (*dash line*)

$$\Delta D = HU + E \tag{4}$$

In Eq. 4, ΔD is a matrix that contains the computed output response (flying height) of the heater:

$$\Delta D = \begin{bmatrix} \Delta d(1) & \Delta d(2) & \cdots & \Delta d(n) \\ \Delta d(2) & \Delta d(3) & \cdots & \Delta d(n+1) \\ \vdots & \vdots & \ddots & \vdots \\ \Delta d(n) & \Delta d(n+1) & \cdots & \Delta d(2n-1) \end{bmatrix} \tag{5}$$

where Δd represents the vector of n considered data points (flying heights) for a given power input step (n represents half or less the total amount of available data points). The input signal to the heater is represented by the upper triangular matrix U consisting of ones, and the thermal actuator discrete model is represented by H, a Hankel matrix that contains the state space matrices A, B and C to be estimated:

$$H = \begin{bmatrix} C \\ CA \\ \vdots \\ CA^{K-1} \end{bmatrix} \begin{bmatrix} B & AB & \cdots & A^{K-1}B \end{bmatrix} \tag{6}$$

The parameter K represents the data point number. The matrix E contains the effect of past output signals:

$$E = \begin{bmatrix} \Delta d(0) & \cdots & \Delta d(0) \\ \vdots & \ddots & \vdots \\ \Delta d(n-1) & \cdots & \Delta d(n-1) \end{bmatrix} \tag{7}$$

Using singular value decomposition, Eq. 4 can be rewritten as:

$$R = HU = \Delta D - E = U \sum V^T \tag{8}$$

The matrix R can be reduced to a rank N matrix R_N (order of the model) as follows:

$$R_N = R_1 R_2 \tag{9}$$

where $R_1 = U_N \sum_N^{1/2}$ and $R_2 = \sum_N^{1/2} V_N^{1/2}$. It can be shown that the state matrix A is equal to:

$$A = R_1^{-1} \bar{R} R_2^{-1} \tag{10}$$

where $\overline{R} = \Delta\overline{D} - \overline{E}$ represents a matrix of elements shifted one sample forward in time, e.g.

$$\Delta\bar{D} = \begin{bmatrix} \Delta d(2) & \Delta d(3) & \cdots & \Delta d(n+1) \\ \Delta d(3) & \Delta d(4) & \cdots & \Delta d(n+2) \\ \vdots & \vdots & \ddots & \vdots \\ \Delta d(n+1) & \Delta d(n+2) & \cdots & \Delta d(2n) \end{bmatrix} \tag{11}$$

The first column of R_2 and the first row of R_1 represent the space matrices B and C respectively. Additional details about the estimation of the heater actuator model dynamics are giving by Boettcher et al. (2011).

Using GRA, we can estimate the dynamics of the heater actuator due to a power input step. First, the time dependent simulation scheme depicted in Fig. 4 is used to simulate the change in flying height as a function of time for a given power input step (FEM solution in Fig. 6). As can be seen in Fig. 6, the computed flying height change exhibits an initial fast response followed by a much slower response. The initial fast response corresponds to a flying height change (displacement) of approximately 2 nm in less than 80 μs, which is fast enough to respond to the flying height variations of the flying height profile depicted in Fig. 5. The TFC slider computed response is very similar to the experimental measurements depicted in Fig. 2 for the change in flying height versus a power step increase. In order to qualitatively compare the computed and experimental flying height responses, GRA was used to estimate a second order model that fits the finite element results in Fig. 6, similar to the model used to fit the flying height measurements depicted in Fig. 2. Although the second order model proved to be a very good fit for the computed TFC slider response, it was found that a third order model (also computed using GRA) provides an even better fit to the FEM response and can be used even more effectively to simulate the dynamics of the heater actuator.

9 Heater power input signal optimization

As described in Boettcher et al. (2011), a convex optimization approach was used to determine the optimal feed forward input signal profile to the heater element. The optimization procedure uses the estimated model for the heater actuator described in the previous section to calculate the time dependent power input profile needed to compensate for the flying height changes depicted in Fig. 5 and therefore obtain a constant flying height. The optimization problem is stated as follows

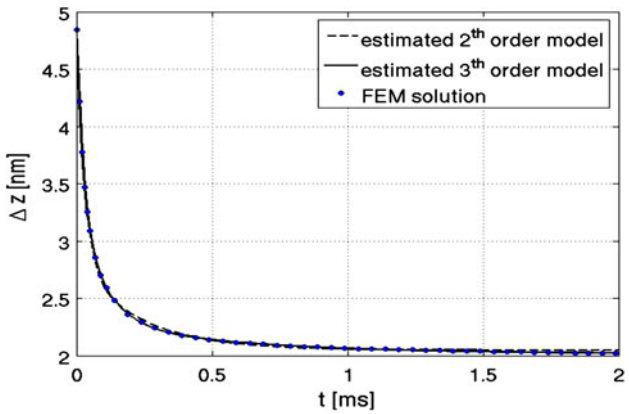

Fig. 6 Computed and estimated time dependent flying height history for a power input step

$$\min_u \|\Psi u + d - \min(d) + z_0\|_2 \tag{12}$$

$$\textit{subject to} \quad \begin{matrix} u \le u_{\max} \\ u \ge u_{\min} \end{matrix}$$

where u represents the input signal to the heater, Ψu the estimated flying height response of the TFC slider as determined by the third order model obtained using GRA, d the values of the simulated flying height profile depicted in Fig. 5, $\min(d)$ the minimum value of d and z_0 an optional additional spacing to position the slider closer to the disk. The convex optimization procedure determines the optimal power input profile to the heater to minimize the Euclidean norm of the expression in Eq. 12. The input signal u cannot be less than zero ($u_{\min}$) or larger than the maximum power input that causes contact with the disk ($u_{\max}$). The optimized power input profile can be seen in Fig. 7. The depicted time dependent power profile is used as input for the heater element in the TFC slider finite element model previously described.

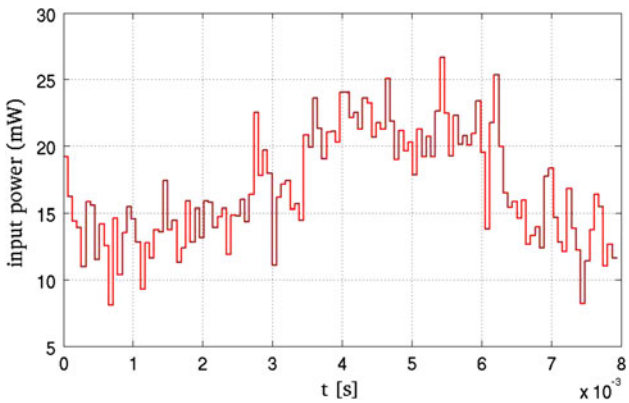

Fig. 7 Heater element power input time dependent history

10 Optimized computed flying height

A time dependent TFC slider/Reynolds equation simulator was used to determine the flying height profile resulting from the optimized power input to the heater element. The optimized flying height profile can be seen in Fig. 8. A spacing of $z_0 = 1.5$ nm was used in addition to the minimum flying height value min(d). The theoretical optimized flying height depicted in Fig. 8 represents the ideal flying height profile that would be obtained if the numerical simulation could be carried out without numerical errors. The small fluctuations observed in the numerical simulation of the optimized flying height profile can be attributed to a combination of numerical round off errors, spatial and temporal discretization errors in the finite element simulation, interpolation errors when mapping heat transfer coefficients and modeling error of the heater actuator dynamics. As can be seen in the statistics presented in Fig. 8, the standard deviation of the computed optimized profile (0.02 nm) is significantly lower than that of the non-optimized profile (0.62 nm). The numerical simulation exhibits less noise and smaller flying height variations than the experimentally optimized flying height profile presented in Fig. 1. The difference between minimum and maximum flying height values for the non-optimized and optimized flying height profiles are shown in Table 2. For the experimentally measured flying height profile depicted in Fig. 1, the maximum difference between flying height measurements before and after optimization was reduced from 2.54 to 0.84 nm. For the case of the numerically simulated flying height profile, the maximum difference between flying height values was reduced from 2.53 to 0.13 nm. The main reason for this large reduction in flying height difference is that the numerical simulation is not affected by experimental noise and measurement error, the latter being significant factors in the experimental data depicted in Fig. 1. Comparing our numerical results with the experimental data, we observe that the computed response reflects very well the flying height response pattern obtained in the experimental investigation. Likewise, the simulation results offer a good qualitative measure of the optimized flying height profile experimentally measured.

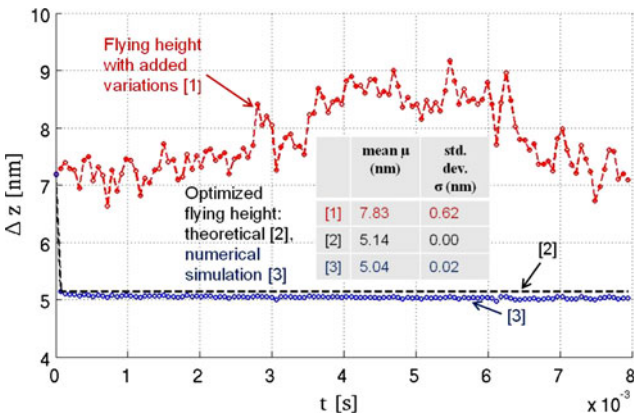

Fig. 8 Initial and optimized flying height time dependent histories

Table 2 Difference between minimum and maximum flying height values for both non-optimized and optimized flying height profiles

	Flying height difference for non-optimized profile (nm)	Flying height difference for optimized profile (nm)
Experimental data	2.54	0.84
Numerical simulation	2.53	0.13

11 Summary

A time-dependent numerical simulation procedure based on the steady state Reynolds equation was implemented to simulate the flying height response of a typical TFC slider. A TFC slider finite element model was implemented in LS-DYNA, a commercially available finite element software. The power input signal to the heater element was optimized to minimize flying height variations using a convex optimization approach. The optimization procedure was applied to a typical experimentally measured flying height profile obtained by Boettcher et al. (2011). Flying height changes were significantly reduced when using the optimized power input signal. It was shown that the time-dependent numerical approach can be successfully used to simulate the experimentally measured response of TFC sliders to power input changes to the heater element. The results from the investigation will be used in future studies to optimize the position and design dimensions of the TFC heater to increase frequency response and minimize repeatable dynamic flying height variations.

References

Boettcher U, Li H, de Callafon RA, Talke FE (2011) Dynamic flying height adjustment in hard disk drives through feed forward control. IEEE Trans Magn 47(1823):1829

de Callafon RA, Moaveni B, Conte JP, He X, Udd E (2008) General realization algorithm for modal identification of linear dynamic systems. J Eng Mech 134(9):712–722

Duwensee M (2007) Numerical and experimental investigations of the head/disk interface. PhD dissertation, University of California, San Diego

Fritzsche J, Li H, Zheng H, Amemiya K, Talke FE (2011) The effect of air bearing contour design on thermal pole-tip protrusion. Mycrosyst Technol 17:813–820

Kurita M, Xu J, Tokuyama M, Nakamoto K, Saegusa S, Maruyama Y (2005) Flying-height reduction of magnetic-head slider due to thermal protrusion. IEEE Trans Magn 41:3007–3009

Li H, Kurita M, Xu JG, Yoshida S (2010) Iteration method for analysis of write-current-induced thermal protrusion. Microsyst Technol 16:161–167

Liu B, Yu SK, Zhou WD, Wong CH, Hua W (2008) Low flying-height slider with high thermal actuation efficiency and small flying-height modulation caused by disk waviness. IEEE Trans Magn 44:145–150

LS-DYNA keyword user's manual (2007) Version 971, Livermore Software Technology Corporation (LSTC)

Song S, Wang L, Rudman V, Fang D, Stoev D, Wang J, Sun B (2007) Finite element analysis of alternating write-current-induced pole tip protrusion in magnetic recording heads. IEEE Trans Magn 43:2217–2219

Wahl M, Lee P, Talke FE (1996) An efficient finite element-based air bearing simulator for pivoted slider bearings using bi-conjugate gradient algorithms. Trib Trans 39(1):130–138

Zhang S, Bogy DB (1999) A heat transfer model for thermal fluctuations in a thin slider/disk air bearing. Int J Heat Mass Transfer 42:1791–1800

Zhou WD, Liu B, Yu SK, Hua W, Wong CH (2008) A generalized heat transfer model for thin film bearings at head-disk interface. Appl Phys Lett 92:043109